Single-Molecule FRET X

Filius, Mike; van Wee, Raman; Joo, Chirlmin

Important note
To cite this publication, please use the final published version (if applicable).
Please check the document version above.

Chapter 10

Single-Molecule FRET X

Mike Filius, Raman van Wee, and Chirlmin Joo

Abstract

Fluorescence resonance energy transfer (FRET) is a photophysical phenomenon that has been repurposed as a biophysical tool to measure nanometer distances. With FRET by DNA eXchange, or FRET X, many points of interest (POIs) in a single object can be probed, overcoming a major limitation of conventional single-molecule FRET. In FRET X, short fluorescently labeled DNA imager strands specifically and transiently bind their complementary docking strands on a target molecule, such that at most a single FRET pair is formed at each point in time and multiple POIs on a single molecule can be readily probed. Here, we describe the sample preparation, image acquisition, and data analysis for structural analysis of DNA nanostructures with FRET X.

Key words Single-molecule FRET, DNA nanotechnology, FRET X, Structural biology, Single-molecule multiplexing

1 Introduction

Owing to its sub-nanometer and millisecond resolution, single-molecule FRET has proven an indispensable tool in the repertoire of biophysicists aiming to elucidate the conformational dynamics and interactions of biomolecules [1]. Moreover, compared to other structural techniques, such as X-ray crystallography and cryo-electron microscopy, sample preparation for FRET experiments is mild, hence the introduction of artefacts is minimal [2]. To measure nanometer distances, the inverse sixth power dependence of the FRET efficiency (E) with respect to the dye separation is employed [3]. However, in conventional single-molecule FRET, the cross talk between different FRET pairs limits the number of FRET pairs that can be analyzed simultaneously to one or two, reducing throughput and maximum complexity of a target

biomolecule [4]. The constraint on the number of FRET pairs is relaxed by our method FRET by DNA eXchange, or FRET X, which employs transient and repetitive binding of short fluorescently labeled DNA strands to its complementary docking strand on a point of interest (POI) [5, 6]. The transient nature of the DNA hybridization ensures temporal separation of FRET pair formation on one molecule, while the repeated probing increases the precision of pair distance determination to a single nucleotide, or 0.01 FRET (E) [5]. Moreover, the highly specific and programmable kinetics of DNA hybridization allow for multiplexed analysis of multiple POIs on a single biomolecule or of different biomolecules through distinguishable binding kinetics or buffer exchange [7–9]. In addition, as fluorophores are continuously replenished from a practically infinite pool, FRET X is essentially immune to photobleaching. This advantageous feature has facilitated extended imaging cycles of several hundreds of seconds to probe a single POI in an individual biomolecule over 20 times while also enabling an increased laser power. Recently, we have implemented our FRET X technology as a tool for protein identification, demonstrating the ability to identify a protein on the basis of its structural fingerprint [10]. Owing to its advantages over conventional single-molecule FRET of an increased precision, higher statistics, photobleaching immunity, and multiplexing possibilities, we envision that the inclusion of FRET X in the structural analysis toolkit will trigger new breakthroughs in single-molecule biophysics. In this chapter, we explicate experimental design, imaging methods, and data analysis procedures.

2   Materials

2.1   Annealing the DNA Nanostructure

1. Annealing buffer: 50 mM Tris–HCl (pH 8.0), 100 mM NaCl, 1 mM $MgCl_2$.
2. ThermoCycler.
3. DNA: the DNA nanostructure in Fig. 2 is built from four individual DNA strands that form a triangular structure with ssDNA overhangs that can be utilized for FRET X imaging (*see* **Note 1**).

2.2   Single-Molecule Imaging

1. Wash buffer (T50): 50 mM Tris–HCl (pH 8.0), 50 mM NaCl.
2. Streptavidin: 0.1 mg/mL streptavidin in T50 buffer.
3. Imaging buffer: 50 mM Tris–HCl (pH 8.0), 500 mM NaCl, 1 mM Trolox, 0.8% dextrose, 0.5 mg/mL glucose oxidase, 85 μg/mL mM catalase (*see* **Note 2**).
4. DNA (biotinylated, and fluorescently labeled, annealed DNA nanostructure, *see* Table 1 and **Notes 3** and **4**).

Table 1
Overview of the DNA sequences of the docking and imager strands and their modifications

DNA Strand	Sequence (5′ – 3′)	Modification
DNA substrate (Fig. 1)	TTTTT TTTTT TTTTT TTTTT ATACATCTAT TTTTT	5′ Cy5, X is biotin-CE at phosphate of 3′
DNA imager strand (Fig. 1)	GATGTAT	3′ Cy3
DNA nanostructure Backbone	ATTCA TTCTC ATCCT CTGTC GGGTG TACCG TAAGG TGAAT AGTGA CTTTA TACAT CTA	
Left arm containing POI A and POI B	AGAGG AGGAT TTCGG TACAC CCGAC AGTTT TCAAT GTA	
Right arm containing POI	TCTTC ATTAC TTTTC ATAAC ATCAG GTCAC TATTC ACCTT A	
Biotin	CTGAT GTTAT GAGGA TGAGA ATGAA TTTTT TTTTT T	3′ biotin
Imager strand POI A (Fig. 2)	TCCTCCT	5′ Cy3
Imager strand POI B (Fig. 2)	AGATGTAT	3′ Cy3
Imager strand POI C (Fig. 2)	TACATTGA	3' Cy3
Acceptor imager strand (Fig. 2)	AGTAATGAA	5′ Cy5

2.3 Data Acquisition and Analysis Software

1. Lab-made software written in Visual C++ for data acquisition.
2. Matlab is used for trace extraction (code available at: https://github.com/kahutia/SingleMoleculeImageAnalyzer/releases/tag/V8.0) for automated FRET X analysis of single-molecule traces (available at: https://github.com/kahutia/transient_FRET_analyzer2) [6].
3. Origin software for data analysis and visualization.

3 Methods

3.1 Single-Molecule Fluorescence Microscopy, Data Acquisition, and Analysis

A custom-built prism-type total internal reflection microscope (prism-TIRFM) is used for the single-molecule experiments [11]. All single-molecule experiments are performed at room temperature (23 ± 1°C).

3.2 Single-Molecule FRET X

1. The quartz slides are passivated and pegylated as described before [11] and then the assembled as described previously [12].

2. Inject 50 μL of T50 to wash the channels.

3. Inject 50 μL of 0.1 mg/mL streptavidin in T50 and incubate for 2 min.

4. Inject 200 μL of T50 to wash out excess streptavidin.

5. Inject 50 μL of 75 pM biotinylated, acceptor (Cy5)-labeled DNA substrate in T50 (Fig. 1a, b) and incubate for 2 min (*see* **Note 5**).

6. Inject 200 μL of T50 to wash out excess biotinylated DNA.

7. Inject 50 μL of imaging buffer containing 10 nM donor (Cy3) labeled FRET X imager strands (Fig. 1a, b, *see* **Note 6**). The base sequence and length (six to eight nucleotides) of the imager strands are chosen such that the bright dwell-time (the time an imager strand is hybridized to the nanosctructure) would be as short as possible to prevent photobleaching, but still long enough (>0.5 s) for accurate determination of the FRET efficiency for each binding event [5] ($\Delta\tau = 0.6 \pm 0.1$ s, Fig. 1d; Movie 1). Similarly, the imager strand sequence, its concentration, and the salt concentration are chosen to decrease the dark dwell time (the time between subsequent imager strand binding events on a single molecule) and hence to maximize the number of FRET events detected within a movie ($\Delta\tau = 13.4 \pm 0.2$ s, Fig. 1e; Movie 1, *see* **Note 7**).

8. The microfluidic device is loaded onto the microscope stage.

9. The sample chamber is illuminated with a 532-nm solid state laser to excite the Cy3 fluorophore. Start with a laser power of 10 mW (6.7 μW/μm^2) and adjust depending on desired signal-to-noise ratio (S/N), the fluorophore's photon budget and the sample's resistance against photodamage [13]. Camera's frame rate is 10 Hz, and experiments typically last for 2000 frames.

10. Donor and acceptor signal are mapped using a slide with fluorescent beads, and single molecules are identified using a maximum intensity projection of both donor and acceptor channel (*see* **Note 8**). Fluorescence intensity time traces are subsequently extracted through IDL software using a custom script (Fig. 1c).

11. For automated detection of individual binding events of the imager strands in the generated time traces, we use a custom MATLAB script [6]. A two-state K-means clustering algorithm is applied on the sum of the donor and acceptor fluorescence intensities of individual molecules to find an adequate intensity threshold to divide the traces into higher or lower intensity segments [6]. The higher intensity segments are then classified
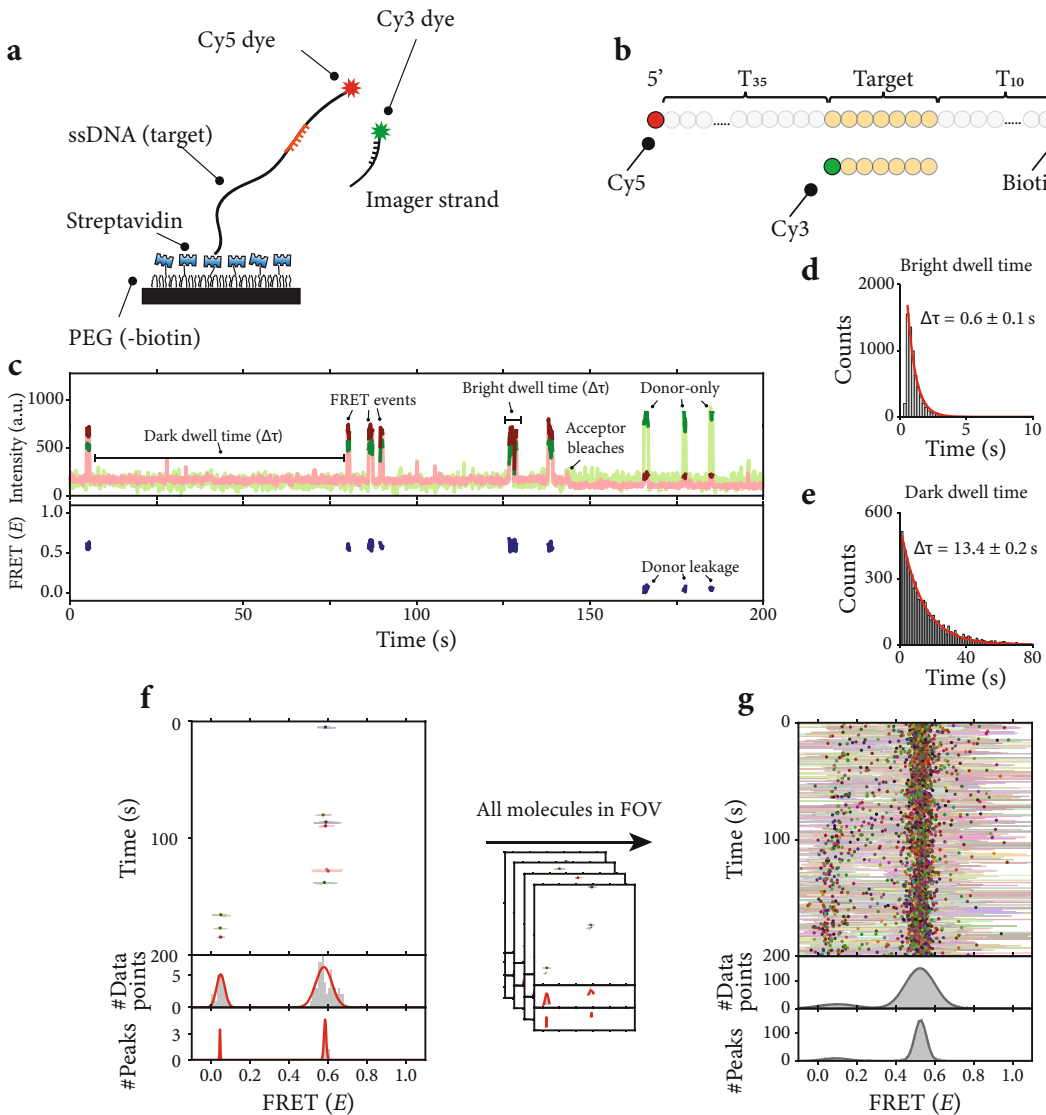
Fig. 1 High-resolution single-molecule FRET using DNA eXchange. (**a**) In a FRET X assay, molecules (in this case single-stranded (ss)DNAs) are immobilized on a PEG-biotin surface through biotin-streptavidin conjugation. The ssDNA contains a donor docking site, which harbors a region complementary to the donor (Cy3, green star)-labeled imager strands in solution. The ssDNA is labeled with an acceptor (Cy5, red star) dye, so upon binding of the donor imager strand, short-lived FRET events are observed. (**b**) Schematic representation of a DNA target construct having a Cy5 dye at one of its ends and a biotin at the other. The target location for binding of the donor imager strand is shown in yellow. (**c**) Typical single-molecule time trace showing both the Cy3 and Cy5 intensity. Short-lived FRET events are observed (top panel) and their FRET efficiency (*E*) is determined (bottom panel). The duration of a FRET event depends on the dwell time ($\Delta\tau$) of the donor imager strand. After the acceptor bleaches ($t = 140$ s), donor-only events are observed, and their partial fluorescence leakage into the acceptor channel is wrongly identified as low FRET (*E*) events. (**d**) The duration of FRET events is referred to as the bright dwell time. The distribution is fitted with a single exponential from which the dwell time (mean $\pm$ standard deviation) is extracted. (**e**) The time in between FRET events is referred to as the dark dwell time. The distribution is fitted with a single exponential from which the dwell time (mean $\pm$ standard deviation) is extracted. (**f**) Left, top panel: single-molecule kymograph of the time trace shown in (**c**). The FRET

as binding events and to reduce false positive detections, only binding events that last for more than three consecutive frames (0.3 s) are selected for further analysis (*see* **Note 9**).

12. The FRET efficiency is calculated for each binding event and used to build the single-molecule FRET kymograph and histogram. Separate peaks in the FRET efficiency histogram are found through Gaussian mixture modeling with one to five peaks per histogram, and then the best fit is selected using the Bayesian information criterion (Fig. 1f). The kymograph shows the FRET efficiency per data point (or frame, Fig. 1f, lines) and the mean FRET efficiency from all data points per binding event (Fig. 1f, dots). The histograms with the FRET efficiencies per data point (Fig. 1f, middle panel) and per binding event (Fig. 1f, bottom panel) show a single FRET population, indicating that imager binding is highly specific for the target hybridization site (*see* **Note 10**). The ensemble kymograph containing all 363 molecules in a single field of view shows a similar mean FRET of 0.53 (Fig. 1g, right). To increase precision of the FRET (E) determination, a histogram that is built from the mean FRET values per binding events (peak FWHM: 0.07) rather than a FRET histogram that is built from the efficiency for each data point (peak FWHM: 0.17) should be used (*see* **Note 11**).

3.3 Single-Molecule FRET X to Probe Multiple Points of Interest in a Single Nanostructure

FRET X is specifically designed to analyze biomolecules or nanostructures with multiple POIs. Owing to the transient hybridization, in which a single POI is unoccupied for most of the time, multiple POIs can be probed one by one. To demonstrate this advantageous feature, we design a DNA nanostructure with one reference point and three additional POIs with orthogonal docking sequences, which cannot be analyzed when probed simultaneously [5]. Furthermore, by also employing transient hybridization of an acceptor imager strand to the reference point, FRET X becomes photobleaching-immune, and the nanostructure can be imaged indefinitely.

1. The four single-stranded DNAs making up the nanostructure (Fig. 2a) are mixed in a molar ratio of 1:2:2:2 (ratio of the biotin strand to the three individual backbone strands) in annealing buffer and the strands are annealed using a thermocycler (from 80 to 4°C with −1°C/cycle for 5 min/cycle and then stored at 4°C for a week).

Fig. 1 (continued) (E) per data point is shown as a line, while the dots indicate the average FRET (E) per FRET event. The FRET (E) is plotted for all data points (middle panel) or average per FRET event (bottom panel) and the distributions are fitted with a Gaussian function (red). (**g**) The ensemble kymograph and fitted distributions for all molecules in a single field of view
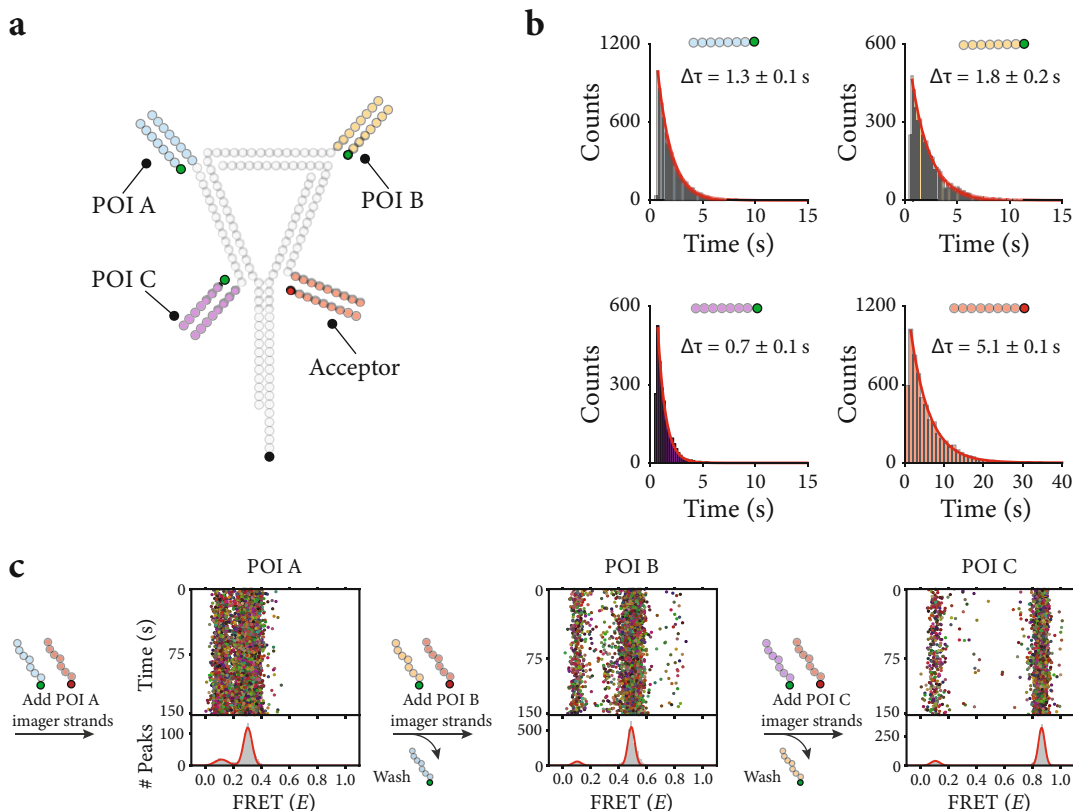
Fig. 2 FRET X analysis of a nanostructure with multiple points of interest. (**a**) Schematic representation of the DNA nanostructure containing three docking sites for three different POIs (purple, blue, and yellow), and one docking strand for the acceptor imager strand (red). (**b**) Dwell-time distributions for all four imager strands fitted with a first order exponential to find their bright dwell time (mean $\pm$ standard deviation). (**c**) Probing the three POIs one at a time in sequential imaging cycles by first adding only the imager strands for POI A, imaging, then washing and then adding the imager strands for the next POI. For each POI, the FRET (*E*) is determined without crosstalk from other POIs and the cycle is repeated until all POIs (three in this example) are probed

2. The microfluidic chamber is prepared as described in the previous section **steps 1–4**. However, to obtain FRET X data for different POIs in the same molecule, the same FOV should be imaged. To this end, we connect tubing to the inlet and outlet of the microfluidic chamber and pull the solution through with a syringe from the outlet to minimize drift during washing and imaging buffer exchange. Next, a solution of 75 pM DNA nanostructure (being the concentration of the biotinylated strand) is immobilized.

3. Each POI consists of an orthogonal FRET X docking strand for which a complementary unique imager strand is present in the imaging buffer (*see* **Note 12**). The different FRET X imager strands are designed to have a dwell time of 1–2 s (Fig. 2b, blue, orange, purple distributions). To avoid the photobleaching of the acceptor dye, we design a unique docking site for the

acceptor imager strand sequence near the 3′ end of the construct (*see* **Note 13**). Yet, to maximize the probability of energy transfer between a donor and acceptor fluorophore, the docking site for the acceptor imager strand should be occupied as much as possible. Thus, the acceptor imager strand is designed to have a longer bright dwell time and shorter dark dwell than the donor imager strands (Fig. 2b, red distribution, *see* **Note 14**).

4. After immobilizing the DNA nanostructures, the imaging buffer consisting of 10 nM donor imager strand for POI A and 50 nM acceptor imager strand (*see* **Note 15**) is injected, and the microfluidic device is loaded onto the microscope stage.

5. The data acquisition is performed as described in the previous section **step 9,** and after obtaining a sufficient number of FRET events per POI (~ 10 binding events per molecule) [5], the microfluidic chamber is washed with 500 μL T50.

6. Next, the imaging buffer containing the imager strand for POI B and the acceptor imager strand is injected, and the FRET X efficiency for POI B is determined. This cycle of imaging buffer exchange and data acquisition can be repeated for an unlimited number of POIs, given they have orthogonal docking strands (Fig. 2c) [7].

7. The data analysis as described in **steps 10–12** of the previous section is then performed separately for each POI.

4   Notes

1. Each of the arms was designed to have a unique docking strand to enable FRET X analysis of each POI one by one. Note that this nanostructure and the sequences used to construct it merely serve as example and that different sequences may be used to design different, more complex nanostructures.

2. The imaging buffer contains 500 mM NaCl to facilitate frequent binding/unbinding of the FRET X imager strands to the point of interest. The dwell times can be further tuned by changing the NaCl concentration or including $MgCl_2$, where an increase in the ionic strength of the buffer leads to an increase in the bright dwell time and a decrease in the dark dwell time, and vice versa.

3. We use the Cy3-Cy5 FRET pair, which has a Förster radius of 5.4 nm [3], but in principle any FRET pair can be used. To probe separations that are significantly smaller or larger than 5.4 nm, different FRET pairs with a matching Förster radius should be used.

4. In the standard design, the DNA imager strands are labeled with fluorophores at their 3′ or 5′ end. However, to alter FRET pair separation without changing the design of the nanostructure, one can also design imager strands having their fluorophore on an internal nucleotide.

5. The concentration of biotinylated DNA is chosen in such a way that the nanostructures are well separated on the EMCCD chip. The maximum number of molecules per FOV is ~500 molecules for our setup (512 × 512 pixels, 60× magnification) but should be scaled accordingly for different magnification and EMCCD chip size.

6. Apart from the salt concentration, the FRET X imager strand concentration influences the binding frequency. The imager strand concentration poses a trade-off between binding frequency and background signal. We chose 10 nM imager strand to maximize the number of binding events (~1 binding per 20 s), while retaining a sufficiently low background signal for accurate FRET (E) determination.

7. The base sequence and the length of the imager strands can be altered for longer or shorter dwell times [14, 15]. Specifically, we recommend to pre-empt possible secondary structure formation by avoiding self-complementary nucleotides in the imager strand and docking strand [15].

8. To facilitate molecule localization, users may briefly excite the Cy5 acceptor to make a reference movie to determine the location of target molecules more efficiently. However, this can only be done when the acceptor fluorophore is permanently present (i.e., hybridized to or conjugated to the immobilized molecules on the surface). Likewise, ALEX can ease peak finding, while also facilitating FRET corrections, provided that the Cy5 background signal is low enough [16].

9. Data analysis can also be performed using any of the available data analysis software packages that are developed by the single-molecule FRET community [17].

10. After ~140 s, the acceptor fluorophore bleaches (as indicated by the drop in Cy5 signal) and FRET can no longer occur, meaning we detect so-called donor-only events. Fluorescence signal leaks into the acceptor channel and in the absence of correction factors to account for this, these events get falsely detected as FRET events with a low efficiency (left peak).

11. This is because fluctuations in FRET efficiency, for example, due to stochastic photophysical and photochemical processes, are averaged out.

12. The precision of FRET efficiency determination is highest when each POI is probed separately. Employing the predictable and programmable nature of DNA hybridization [9], orthogonal imager/docking pairs can be designed for each POI.

13. To reduce interactions between the fluorophore (both donor and acceptor) and the biomolecule, especially when the target molecule is a protein, a chemical linker or DNA sequence serving as spacer may be added between the docking sequence and the target molecule. Beneficially, this will also reduce the depletion of docking strands [13].

14. Still, occasionally there might not be an acceptor imager strand hybridized to the nanostructure at the time a donor imager strand binds, resulting in donor-only events (*see* **Note 10**).

15. To further increase the probability of energy transfer between donor and acceptor fluorophores, the acceptor imager strand concentration is as high as permitted by the minimally required S/N ratio, which is empirical, and is generally around 4 [17]. Typically, a fivefold excess is used, but this may differ per setup.

Declaration of Interests

C.J. and M.F. hold a patent on single-molecule FRET for protein characterization (patent number: WO2021049940).

References

1. Sasmal DK, Pulido LE, Kasal S, Huang J (2016) Single-molecule fluorescence resonance energy transfer in molecular biology. Nanoscale 8:19928–19944. https://doi.org/10.1039/c6nr06794h

2. Wang H-W, Wang J-W (2017) How cryo-electron microscopy and X-ray crystallography complement each other. Protein Sci 26 (1):32–39. https://doi.org/10.1002/pro.3022

3. Lerner E, Barth A, Hendrix J et al (2021) FRET-based dynamic structural biology: challenges, perspectives and an appeal for open-science practices. elife 10. https://doi.org/10.7554/eLife.60416

4. Algar WR, Hildebrandt N, Vogel SS, Medintz IL (2019) FRET as a biomolecular research tool — understanding its potential while avoiding pitfalls. Nat Methods 16:815–829. https://doi.org/10.1038/s41592-019-0530-8

5. Filius M, Kim SH, Severins I, Joo C (2021) High-resolution single-molecule FRET via DNA eXchange (FRET X). Nano Lett 21:3295–3301. https://doi.org/10.1021/acs.nanolett.1c00725

6. Kim SH, Kim H, Jeong H, Yoon TY (2021) Encoding multiple virtual signals in DNA barcodes with single-molecule FRET. Nano Lett 21:1694–1701. https://doi.org/10.1021/acs.nanolett.0c04502

7. Jungmann R, Avendaño MS, Woehrstein JB et al (2014) Multiplexed 3D cellular super-resolution imaging with DNA-PAINT and Exchange-PAINT. Nat Methods 11:313–318. https://doi.org/10.1038/nmeth.2835

8. Wade OK, Woehrstein JB, Nickels PC et al (2019) 124-color super-resolution imaging by engineering DNA-PAINT blinking kinetics. Nano Lett 19:2641–2646. https://doi.org/10.1021/acs.nanolett.9b00508

9. van Wee R, Filius M, Joo C et al (2021) Completing the canvas: advances and challenges for DNA-PAINT super-resolution imaging. Trends Biochem Sci 0:918. https://doi.org/10.1016/J.TIBS.2021.05.010

10. de Lannoy CV, Filius M, van Wee R et al (2021) Evaluation of FRET X for single-molecule protein fingerprinting. iScience 24:103239. https://doi.org/10.1016/J.ISCI.2021.103239

11. Joo C, Ha T (2012) Single-molecule FRET with total internal reflection microscopy. Cold

Spring Harb Protoc 7:1223–1237. https://doi.org/10.1101/pdb.top072058

12. Chandradoss SD, Haagsma AC, Lee YK et al (2014) Surface passivation for single-molecule protein studies. J Vis Exp: JoVE 86:4–11. https://doi.org/10.3791/50549

13. Blumhardt P, Stein J, Mücksch J et al (2018) Photo-induced depletion of binding sites in DNA-paint microscopy. Molecules 23:3165. https://doi.org/10.3390/molecules23123165

14. Schnitzbauer J, Strauss MT, Schlichthaerle T et al (2017) Super-resolution microscopy with DNA-PAINT. Nat Protoc 12:1198–1228. https://doi.org/10.1038/nprot.2017.024

15. Schueder F, Stein J, Stehr F et al (2019) An order of magnitude faster DNA-PAINT imaging by optimized sequence design and buffer conditions. Nat Methods 16:1101–1104. https://doi.org/10.1038/s41592-019-0584-7

16. Hohlbein J, Craggs TD, Cordes T (2014) Alternating-laser excitation: single-molecule FRET and beyond. Chem Soc Rev 43(4), 1156–1171. https://doi.org/10.1039/c3cs60233h

17. Götz M, Barth A, Bohr SS-R et al (2022) A blind benchmark of analysis tools to infer kinetic rate constants from single-molecule FRET trajectories. Nat Commun 13:5402. https://doi.org/10.1038/s41467-022-33023-3